RSC Advances

REVIEW

View Article Online
View Journal | View Issue

Cite this: *RSC Adv.*, 2021, **11**, 7552

Chemistry of porphyrins in fossil plants and animals

Mariam Tahoun,[a] Carole T. Gee,[bc] Victoria E. McCoy,[d] P. Martin Sander[b] and Christa E. Müller*[a]

Porphyrins are macrocyclic tetrapyrrole derivatives that are widely distributed in nature. They are often complexed with a metal ion located in the center of the ring system and may be modified by various substituents including additional rings, or by ring opening, which leads to a plethora of different functions. Due to their extended conjugated aromatic ring system, porphyrins absorb light in the visible range and therefore show characteristic colors. Well-known natural porphyrins include the red-colored heme present in hemoglobin, which is responsible for blood oxygen transport, and the chlorophylls in some bacteria and in plants which are utilized for photosynthesis. Porphyrins are mostly lipophilic pigments that display relatively high chemical stability. Therefore, they can even survive hundreds of millions of years. The present review article provides an overview of natural porphyrins, their chemical structures, and properties. A special focus is put on porphyrins discovered in the fossil record. Examples will be highlighted, and information on their chemical analysis will be provided. We anticipate that the development of novel analytical methods with increased sensitivity will prompt new discoveries of porphyrins in fossils.

Received 20th December 2020
Accepted 8th February 2021

DOI: 10.1039/d0ra10688g

rsc.li/rsc-advances

Introduction

Porphyrins are natural pigments that can be bound to proteins such as cytochromes and hemoglobin and are found in a huge variety of organisms. Their major structural features have remained detectable for up to 1.1 billion years.[1] For these reasons, they are considered important indicators of life and have been studied from the remains of extinct organisms to understand the principles of evolution.[2,3] Porphyrins are found either isolated in sediments, oil shales, and petroleum,[4] or bound to a fossil tissue. While the findings and structural features of sedimentary porphyrins have been extensively discussed,[5–11] reviews on porphyrins extracted from fossil tissues are lacking. This review article aims to describe the major porphyrins found in fossil plants and animals, and to compare them to natural porphyrins well-known in the present-day world such as heme, chlorophylls, and bacteriochlorophylls.

General structure of porphyrins and their derivatives

Porphyrins are conjugated tetrapyrrole macrocycles linked together by methine (=CH–) bridges. The basic, unsubstituted structure is called porphin (**1**) shown in Fig. 1 along with the current numbering system for porphyrins.[4,12] The pyrrole rings are lettered from A to D.[1] Common side chains attached to porphyrins include methyl, ethyl, vinyl, acetic acid, and propionic acid. The carbon bridges connecting the pyrrole rings are called *meso*-positions and are sometimes designated α-, β-, δ-, and γ-positions. Isomers frequently occur and are identified by adding Roman numerals at the end of the name. Porphyrins readily form complexes with metal cations such as iron(II/III), magnesium(II), copper(II), and zinc(II) to yield metalloporphyrins.[13] Compounds related to porphyrins with saturated bonds and/or extra rings exist that include chlorin (**2**), phorbin (**3**), bacteriochlorin (**4**), and their derivatives (Fig. 1).[4,14] Chlorin (**2**) is 17,18-dihydroporphin[1] while phorbin (**3**) is a chlorin derivative containing an extra isocyclic ring between ring C and D. Bacteriochlorin (**4**) represents a 7,8,17,18-tetrahydroporphin derivative. If a methine bridge between ring A and ring D is cleaved, open-chain tetrapyrroles (bilanes, **5**, Fig. 1) are formed.[4] Their numbering is similar to that of porphins with the *meso*-positions lettered a, b, and c. If there are one, two or three double bonds at the *meso*-positions, the corresponding derivatives are named bilenes, biladienes or bilatrienes, respectively.

Physicochemical properties of selected porphyrins

Porphyrins are aromatic and have a square planar geometry. There are 22 π-electrons present, 18 of which are involved in delocalization, while two electron pairs of nitrogen atoms are sterically hindered when bound to hydrogen, in accordance with Hückel's rule.[4,15] The conjugated double bonds of

[a]*Pharmaceutical Institute, Pharmaceutical & Medicinal Chemistry, University of Bonn, An der Immenburg 4, 53121 Bonn, Germany. E-mail: christa.mueller@uni-bonn.de*
[b]*Institute of Geosciences, Division of Paleontology, University of Bonn, Nussallee 8, 53115 Bonn, Germany*
[c]*Huntington Botanical Gardens, 1151 Oxford Road, San Marino, California 91108, USA*
[d]*Department of Geosciences, University of Wisconsin-Milwaukee, 3209 N Maryland Ave, Milwaukee, WI, 53211, USA*

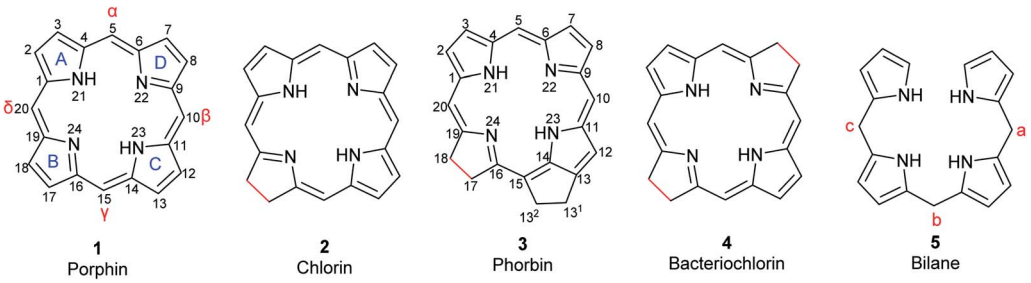

Fig. 1 Basic structures of tetrapyrrole macrocycles from which the natural pigments are derived. Differences in bond saturation are highlighted in red. The current numbering system for porphin and phorbin are shown.

Table 1 Physicochemical properties of selected porphyrin-based pigments[12,16,17,19–21]

Pigment[a]	Molecular formula	Molecular weight (g mol^{-1})	UV-vis absorption maxima (nm)		Color in solution
			Soret	Q-bands	
Heme	$C_{34}H_{32}FeN_4O_4$	616.5	416[b]	520, 550[b]	Red
Hemin	$C_{34}H_{34}ClFeN_4O_4$	654.0	363, 385[c]	550, 570[c]	Olive-green
Hematin	$C_{34}H_{34}FeN_4O_5$	634.5	364, 383[c]	613[c]	Dark blue-brown
Biliverdin	$C_{33}H_{34}N_4O_6$	582.7	376[c]	671[c]	Blue-green
Bilirubin	$C_{33}H_{36}N_4O_6$	584.7	452[c]	—	Yellow-orange
Protoporphyrin IX	$C_{34}H_{34}N_4O_4$	562.7	400[d]	506, 532, 580, 630[d]	Red-brown
Chlorophyll *a*	$C_{55}H_{72}MgN_4O_5$	893.5	430[e]	662[e]	Yellow-green
Chlorophyll *b*	$C_{55}H_{70}MgN_4O_6$	907.5	453[e]	642[e]	Blue-green
Chlorophyll c_1	$C_{35}H_{30}MgN_4O_5$	611.0	444[e]	577, 626[e]	Blue-green
Chlorophyll c_2	$C_{35}H_{28}MgN_4O_5$	609.0	447[e]	580, 627[e]	Blue-green
Chlorophyll c_3	$C_{36}H_{28}MgN_4O_6$	637.0	452[e]	585, 627[e]	Blue-green
Bacteriochlorophyll *a*	$C_{55}H_{74}MgN_4O_6$	911.5	388	805, 870	Blue-green

[a] For structures, see Fig. 2, 3, 6, and 7. [b] Measured in extracts of mitochondrial cytochrome *c* from a horse's heart. [c] Measured in 1 M phosphate-buffered saline (PBS) containing 30 mM NaOH (hemin), 7.2 mM KOH (bilirubin) or 5 mM KOH (biliverdin). [d] Measured in a mixture of acetonitrile and DMSO (3 : 1, v/v). [e] Measured in diethyl ether.

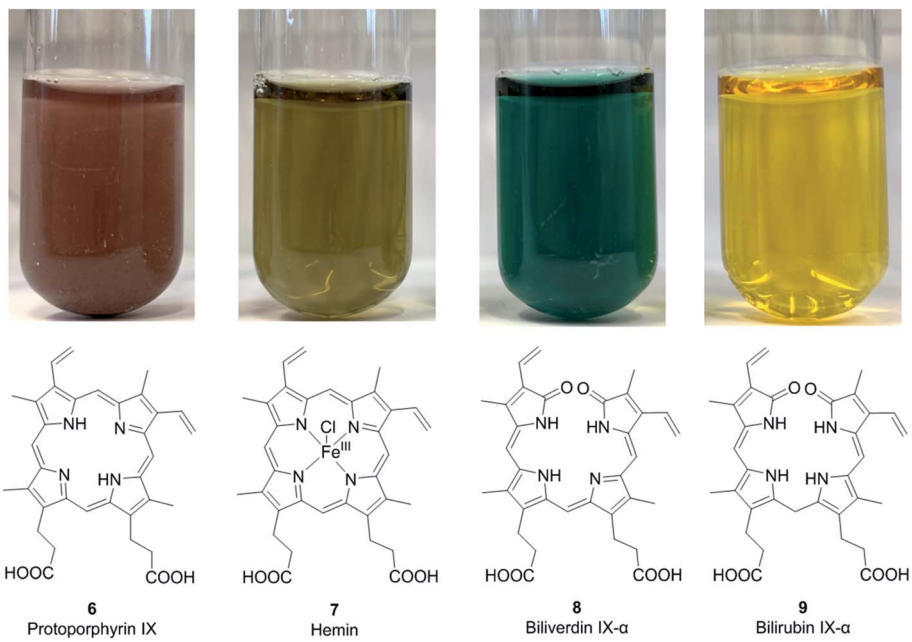

Fig. 2 Structures and colors of protoporphyrin IX (**6**), the metalloporphyrin hemin (**7**), and the open-chain tetrapyrrole derivatives biliverdin IX-α (**8**) and bilirubin IX-α (**9**) in aqueous solution (100 μM concentration).

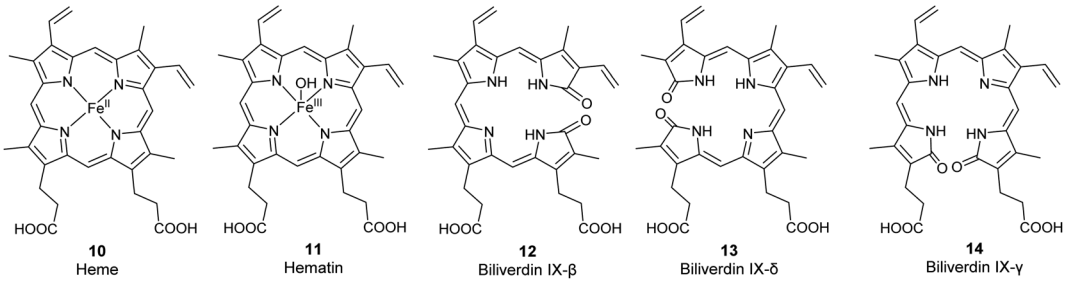

Fig. 3 Structures of the metalloporphyrins heme (**10**) and hematin (**11**) and of the less common biliverdin isomers β, δ, and γ (**12–14**).

porphyrins make them absorb light at defined wavelengths, resulting in a colorful appearance.[4] The electronic absorption spectra of porphyrins are characterized by two prominent bands in the UV region and the visible region. The major band around 400 nm, called the Soret band, appears due to π–π* transitions of the delocalized electrons. This band is characteristic for porphyrins and used for quantification using UV-vis spectrophotometry.[4,16] The Soret band becomes less intense if conjugation is lost and/or the ring is cleaved. In the visible region, there are Q-bands that arise from π–π* transitions of the conjugation between unsaturated carbons and the pyrrole nitrogens.[4,17] Even in the presence of saturation in ring B, chlorin, phorbin, and bacteriochlorin derivatives still possess the 18 π-electrons necessary for delocalization. They have similar spectra as porphyrins and are green in color. Their Soret bands occur in the region from 380–420 nm due to macrocyclic conjugation, while their Q-bands in the range of 500–800 nm are responsible for their vibrant verdant color (Table 1).[18]

Porphyrins identified in fossil tissues

Many exceptionally well-preserved fossil hard and soft tissues, such as digestive organs, eggshells, red blood cells, bone osteocytes, and muscle cells, have been morphologically described with major macromolecules, mostly occurring as structural proteins. However, very few have been chemically analyzed for small organic molecular components.[22] The field of "molecular paleontology" investigates fossil organisms for small organic molecules or their diagenetic products using a combination of analytical techniques.[23] Macromolecules are often investigated by microscopic and immunological techniques. Small organic molecules in fossils are usually extracted using suitable techniques, then analyzed using gas chromatography (GC) or high-performance liquid chromatography (HPLC) and quantified by UV-vis spectroscopy or mass spectrometry. If these molecules are not extractable, non-destructive techniques such as Raman or infrared spectroscopy are used to identify specific chemical signals.

Organic molecules that resist decay are either inherently stable in their surrounding environment or are shielded from degradation by embedding within the core of the preserved macromolecules through various chemical mechanisms. Highly hydrophobic molecules such as sterols and porphyrins have a higher chance of being preserved than more polar compounds. Minimal alterations

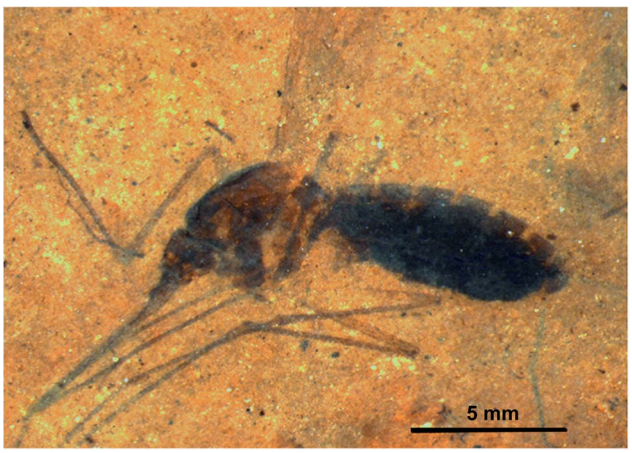

Fig. 4 The oldest female fossil mosquito (*Culiseta* species, 46 million years old) from the middle Eocene Kishenehn Formation in northwest Montana with blood in its abdomen. Heme (**10**) was identified in the abdomen by time-of-flight secondary-ion mass spectrometry and elemental analysis using energy-dispersive X-ray spectroscopy. Scale bar: 5 mm. Image reproduced with permission from D. E. Greenwalt.[28]

Fig. 5 Clutch of fossil oviraptorid dinosaur eggs from Upper Cretaceous sediments of southern China. Protoporphyrin IX (**6**) and biliverdin (**8**) were identified from these fossils using HPLC-ESI-MS and qTOF-MS, and confirmed by similar retention times and exact mass to those of standard samples, whereas these peaks were not found in samples from the surrounding sediment.[38] Photo by Tzu-Ruei Yang, National Museum of Natural Science, Taiwan.

of the structures may occur, such as loss of functional groups (*e.g.*, hydrolysis of esters), reduction, isomerization, aromatization, or condensation. Moreover, on the macromolecular level, several mechanisms also play a role in preservation. For instance, the compact tertiary structures of myoglobin and hemoglobin are stabilized by hydrogen bonding and disulfide linkages, reducing exposure to water and degradative enzymes. In other cases, minerals can be deposited around proteins such as collagen, thereby blocking interstitial spaces and hindering the movement of water and microorganisms.[23,24]

Regardless of the mechanism, initial preservation must occur before complete decay, which may range from hours to days depending on the tissue type. Afterwards, other factors come into play to maintain the integrity of the fossil. For example, compression of the fossil by the sediment preserves integrity and, on the chemical level, promotes cross-linking with macromolecules because the molecules are brought closer to one another.[23]

Heme

The most common biologically relevant metalloporphyrin is heme (**10**, Fig. 2), the ferrous [Fe(II)] complex of protoporphyrin IX (**6**, Fig. 3).[4] Fe(II) has a coordination number of 6 in most of its complexes. In free heme, only four complex bonds are formed with the four pyrrole nitrogen atoms of the porphyrin macrocycle, resulting in a planar complex. In hemoglobin, the iron(II) center of heme is additionally bound to a histidine residue of the protein globin and to oxygen (O_2), resulting in an octahedral complex. Hemoglobin and the related myoglobin are the main proteins responsible for oxygen transport in blood and storage in muscle, respectively. Other hemoproteins include cytochromes (*e.g.*, the cytochrome P450 enzymes and the respiratory cytochromes), and the enzymes catalase, peroxidase, tryptophan pyrrolase, and NO synthase. Free heme is kept at very low concentrations because it is involved in free-radical formation and can oxidize biomolecules. In addition, it may accumulate in cellular membranes due to its high hydrophobicity by which it could damage the phospholipid bilayer. Heme is responsible for the red color of blood.[12,16]

Hemin and hematin. The corresponding ferric [Fe(III)] complexes with **6**, hemin **7** and hematin (**11**, Fig. 2), have an overall positive charge and thus associate with chloride and hydroxide ions, respectively. They are commercially available as stable precursors of heme used as analytical standards.[12,16] Hematin (**11**) is formed from **7** in aqueous alkaline solutions and is a cofactor of peroxidases and cytochromes. Hemin (**7**) acts as an allosteric regulator of heme biosynthesis by inhibiting the enzyme δ-aminolevulinic acid (ALA) synthase.[25] It is also used for the treatment of acute porphyrias in individuals with defective heme biosynthesis.[26]

Heme in the fossil record. Heme (**10**) was previously characterized from the *ca.* 66 million year-old bones of *Tyrannosaurus rex* from the Upper Cretaceous Hell Creek Formation of eastern Montana, USA, by several analytical methods. Bone extracts analyzed

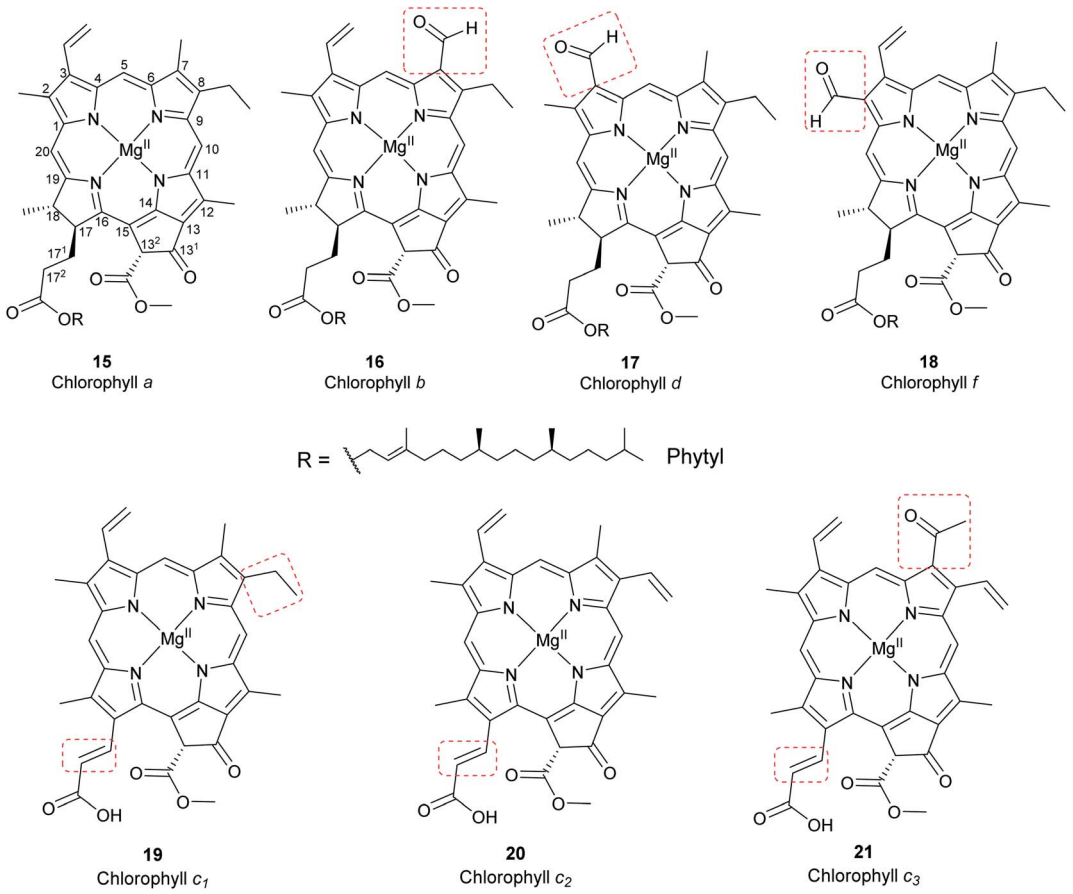

Fig. 6 Structures of the known chlorophylls.

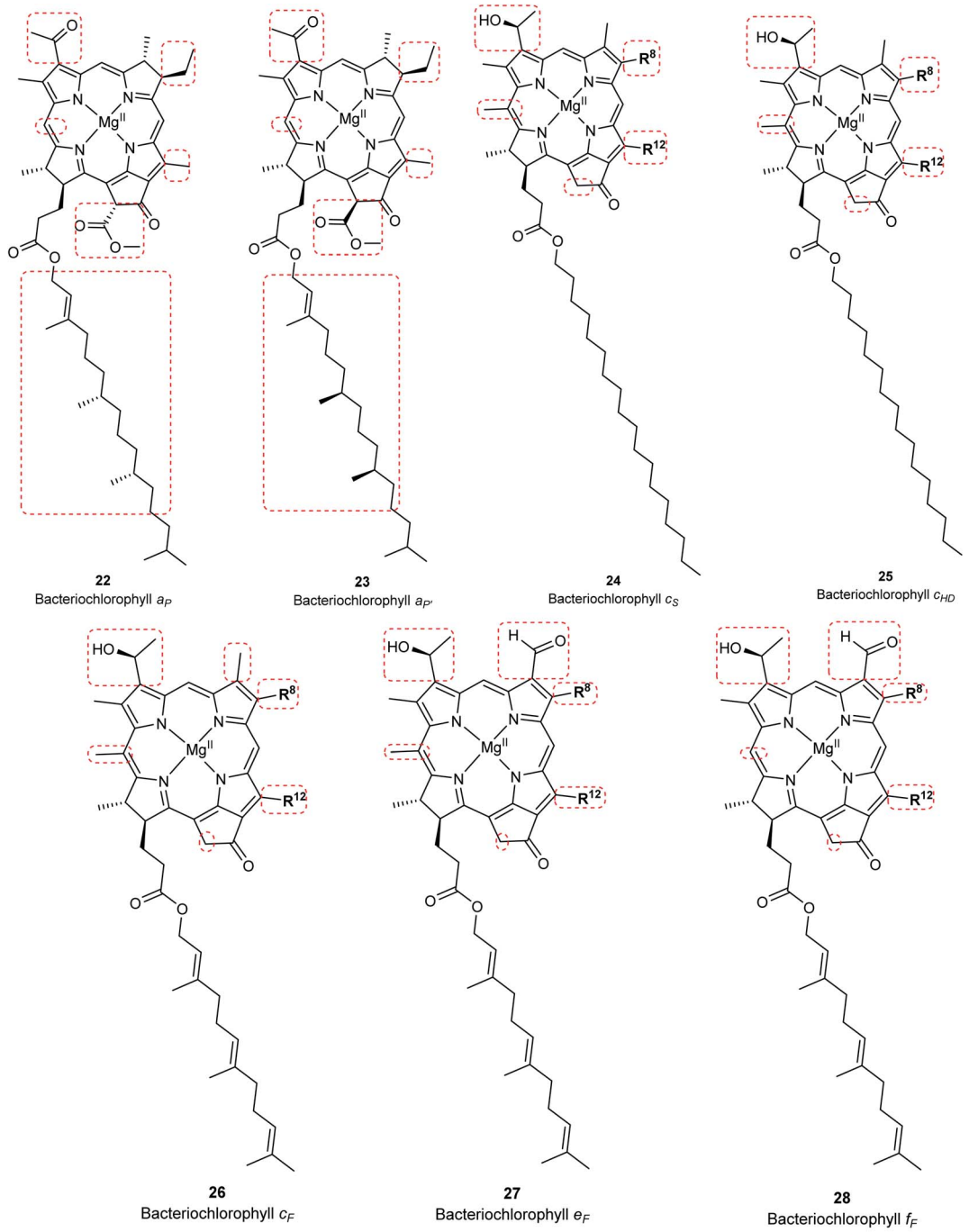

Fig. 7 Structures of bacteriochlorophylls and *Chlorobium* chlorophylls.

using UV-vis spectroscopy showed a Soret absorption peak at 410 nm, which was absent in control and sediment samples. ^{1}H-NMR analyses showed that the iron atom was in the ferric [Fe(III)] state, indicating oxidation might have occurred during diagenesis. Resonance Raman analyses displayed four of the six characteristic bands for **10** confirming its presence.[27]

Compound **10** was indirectly detected in the abdomen of 46-million-year-old female mosquitoes (*Culiseta* spp., Fig. 4) from the middle Eocene Kishenehn Formation in northwest Montana. These were the first fossils of its kind to be identified. Elemental analysis using energy-dispersive X-ray spectroscopy showed an eightfold elevation in iron levels in the abdomen compared to the thorax. Since only female mosquitoes ingest blood,

this iron was thought to originate from the degradation of hemoglobin in their abdomen. In comparison, the iron levels in the abdomen of fossil male mosquitoes were found to be as low as those in the female mosquitos' thorax. Using time-of-flight secondary ion mass spectrometry (ToF-SIMS), other forms of iron such as pyrite (FeS_2) or siderite ($FeCO_3$), normally present in surrounding sediments, were not detected in the fossil confirming, that the source of iron was endogenous. Intact **10** in the fossil was not detected by ToF-SIMS compared to controls of purified hemoglobin, but the fragmentation patterns were very similar. Given the high iron levels, this was expected. Analyses of surrounding sediment and the abdomen of male fossil mosquitoes showed different fragmentation patterns.[28]

Fragments of **10** were detected in fossil sea turtles (*Tasbacka danica*, at least 54 million years old) with soft-tissue preservation from the marine sediments of the early Eocene Fur Formation in Jütland, Denmark. ToF-SIMS analysis showed similar fragmentation patterns when compared with standard samples of hemin and related porphyrins such as **6** and **15**. These molecular analyses were complementary to immunological techniques carried out, which showed a positive reaction after the addition of antibodies against alligator and ostrich hemoglobin.[29]

Degradation products of heme: biliverdin and bilirubin

As the life span of red blood cells nears their end, **10** is degraded by heme oxygenase, which oxidizes and subsequently cleaves **10** at an interpyrrolic position, preferably at the α-position,[30] to form biliverdin IX-α **8** (Fig. 2), a hydrophilic, blue-green bilatriene pigment. Carbon monoxide and Fe(II) are released as side products, and the iron is recycled for heme production. Compound **8** is responsible for the blue-green coloration in the eggshells of many birds.[30,31] As ring opening can occur at any of the interpyrrolic positions in heme, four biliverdin isomers can be formed: biliverdin-IX α, β, δ, and γ (Fig. 2 (**8**) and 3 (**12–14**)). Biliverdin is immediately reduced at another interpyrrolic position to the hydrophobic yellow pigment, bilirubin IX-α (**9**, Fig. 2), a biladiene, by the enzyme biliverdin reductase, which is present in all tissues but most active in the liver and spleen.[32] Bilirubin is later conjugated with glucuronic acid and excreted in bile.[16,33,34]

Protoporphyrin IX

Protoporphyrin IX (**6**, Fig. 2) is a major precursor of chlorophyll and the immediate precursor of heme biosynthesis. The compound bears two carboxylic acid groups and is liable to oxidation.[4,17]

Protoporphyrin IX and biliverdin in the fossil record. As the major pigments responsible for eggshell color,[31,35] protoporphyrin IX (**6**) and biliverdin (**8**) were detected in several extinct avian species using both destructive and nondestructive techniques. Samples were analyzed after extraction from subfossil upland moa eggshell fragments from New Zealand using HPLC-ESI ion trap mass spectrometry,[36] and nondestructively using Raman spectroscopy confirmed by micro-time-of-flight-ESI-MS (micro-TOF-ESI-MS).[37]

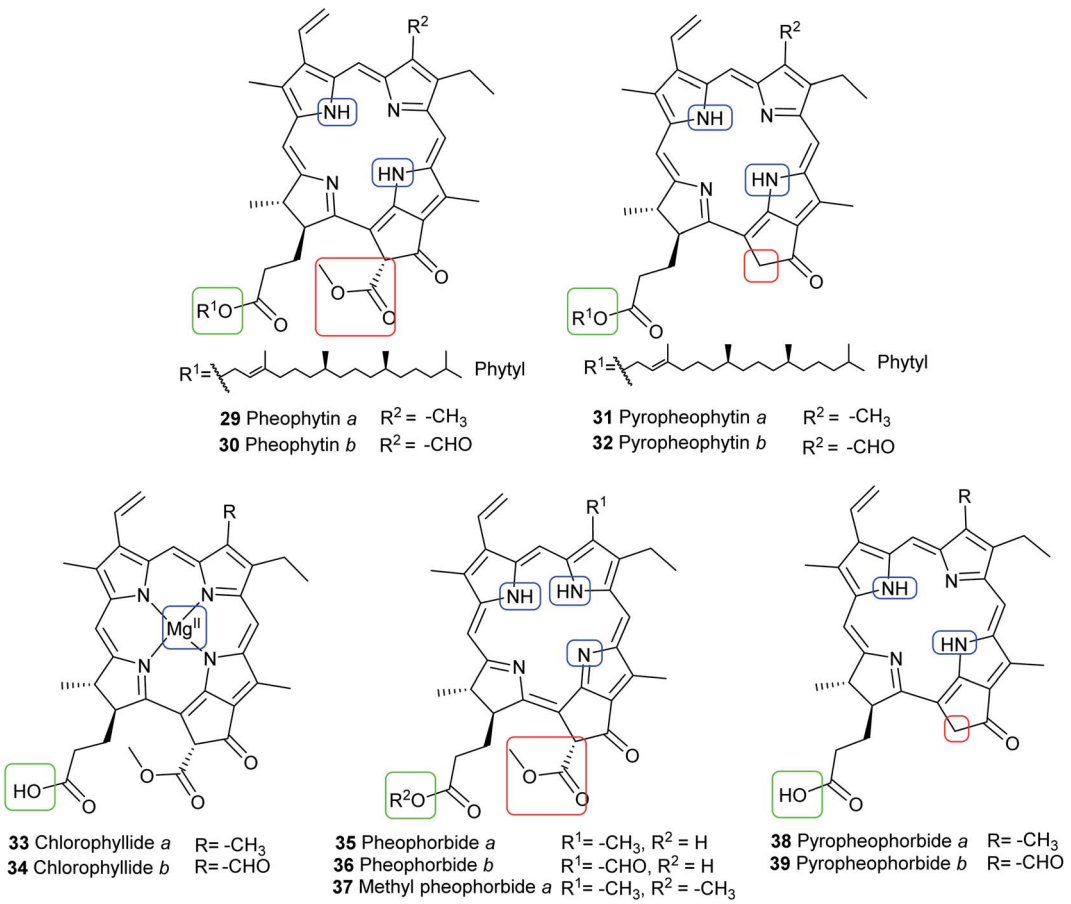

Fig. 8 Structures of chlorophyll metabolites with intact macrocycles.

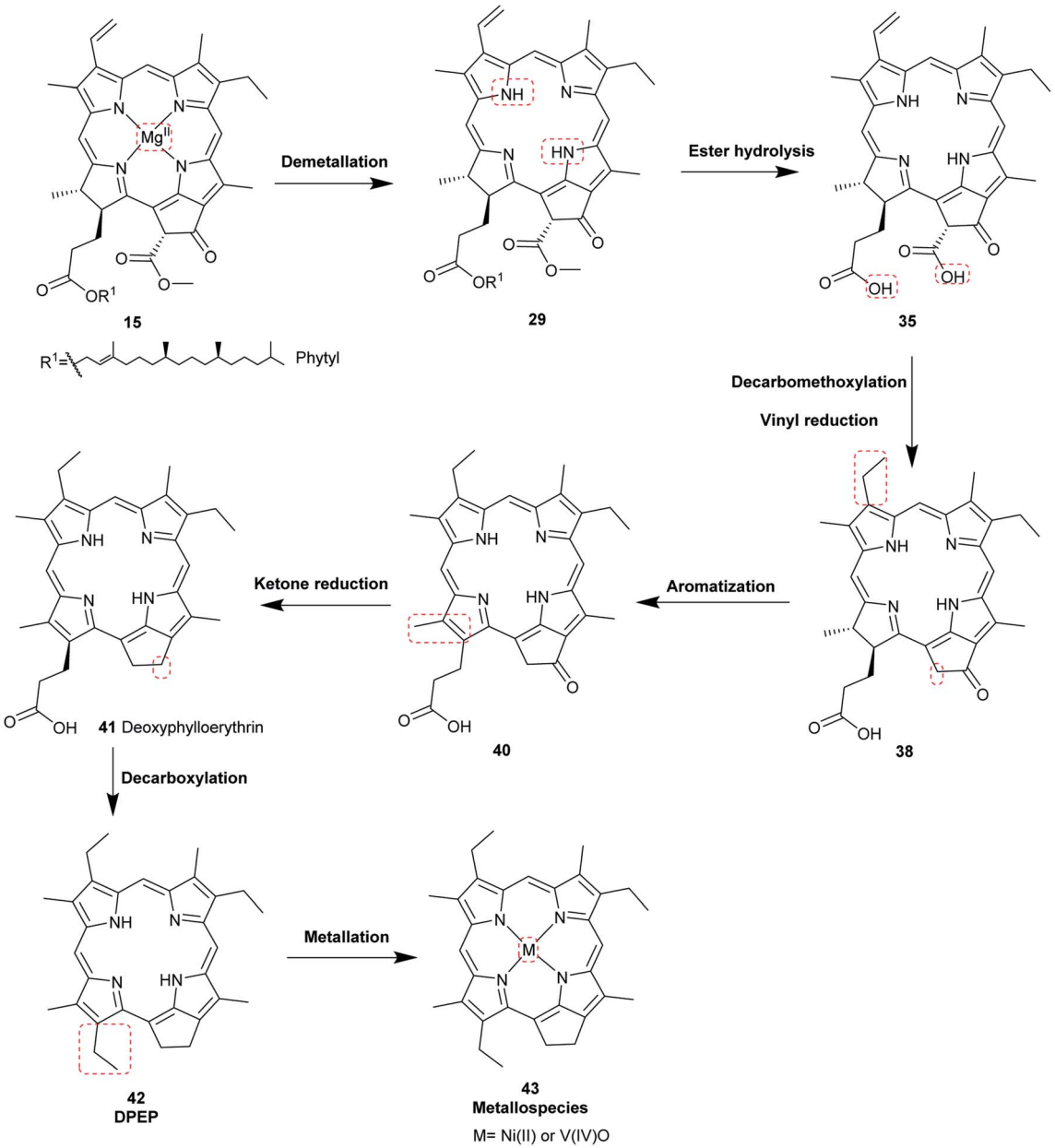

Fig. 9 Diagenetic changes of chlorophyll *a* (**15**) as proposed by A. E. Treibs.[49]

Furthermore, the protoporphyrin IX (**6**) and biliverdin (**8**) were identified from dark gray to slightly greenish colored fossil eggshells of the oviraptorid dinosaur *Heyuannia huangi* (Fig. 5) from the Upper Cretaceous deposits (66 million years old) in eastern and southern China using HPLC-ESI-MS and qTOF-MS, confirmed by similar retention times and exact mass to those of standard samples, whereas the peaks were not found in samples from the surrounding sediment.[38]

Chlorophylls

Chlorophylls are natural pigments found in higher plants, photosynthetic algae, and cyanobacteria. They are classified as chlorophylls (Fig. 6), bacteriochlorophylls, and *Chlorobium* chlorophylls (Fig. 7). The magnesium(II) complexes derived from phorbin include chlorophyll *a* (**15**), chlorophyll *b* (**16**), chlorophyll c_1 (**19**), chlorophyll c_2 (**20**), chlorophyll c_3 (**21**), chlorophyll *d* (**17**), chlorophyll *f* (**18**),[14,39] and the bacteriochlorophylls **22–28**, all of which feature a 5-membered carbocyclic ring fused to ring C of the porphyrin core structure (Fig. 6 and 7).

Chlorophyll *a* (**15**) is the major pigment involved in the photosynthesis in higher plants, algae, and cyanobacteria. Chlorophyll *b* (**16**) is typically present together with **15** at a ratio of 1 : 3.[4] The prominent chlorophylls in photosynthetic bacteria and algae are **19–21**, whereby the red-shifted chlorophylls *d* (**17**) and *f* (**18**) are only present in some cyanobacteria.[40–43] Bacteriochlorophylls are found in anaerobic bacteria,[43,44] most of which are depicted in Fig. 7. They differ in the parent structure from which they are derived. Compound **22** is the most abundant, while **24–28** are only found naturally in green bacteria

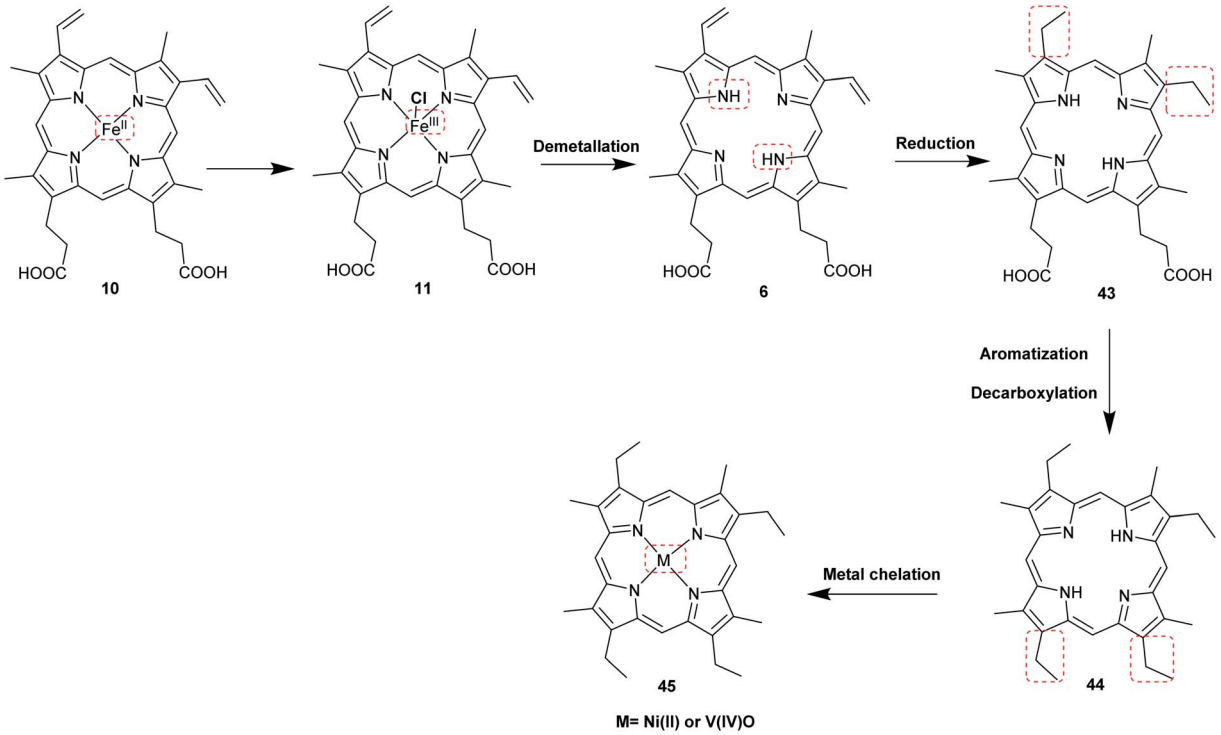

Fig. 10 Diagenetic changes of heme (**10**) as proposed by A. E. Treibs.[9,11,49]

such as *Chlorobium* and *Chloropseudomonas* and are sometimes separately classified as *Chlorobium* chlorophylls.[45]

Degradation products of chlorophylls

Chlorophyll metabolites with intact macrocycle. *In vivo*, chlorophylls are enzymatically degraded by chlorophyllase which is present in all photosynthetic tissues. Ester hydrolysis occurs, forming chlorophyllide *a* (**33**) and chlorophyllide *b* (**34**) from chlorophyll *a* (**15**) and chlorophyll *b* (**16**), respectively. Chlorophyllides are green in color and are more hydrophilic than their parent chlorophylls because the hydrophobic long-chain phytol is removed. A magnesium-dechelating enzyme (Mg dechelatase) leads to demetallation, forming pheophorbide *a* (**35**) and pheophorbide *b* (**36**), which are blue or dark brown to black in color. Additionally, the brown-colored pheophytin *a* (**29**) and pheophytin *b* (**30**) can be formed if magnesium dechelatase acts directly on **15** or **16**. These metabolites are commonly formed during senescence of leaves in the autumn and winter months or as by-products during the extraction process.[46–48] Heat results in formation of pyropheophorbide *a* (**38**) and pyropheophorbide *b* (**39**), pyropheophytin *a* (**31**), and pyropheophytin *b* (**32**).[43] The structures of chlorophyll metabolites bearing an intact phorbin ring are shown in Fig. 8.

Proposed diagenesis of heme and chlorophyll *a* with evidence from sedimentary porphyrins

The most common porphyrin found in sediments is deoxophylloerythroetioporphyrin (**42**, DPEP, Fig. 9), a cyclic alkylporphyrin. In the 1930s, the late organic geochemist Alfred E. Treibs extensively studied **42** and proposed that it originated from chlorophyll *a* (**15**) *via* diagenesis after decay of its biological origin.[9,49,50] He suggested a set of reactions that must have happened to convert **15** into **42**, as shown in Fig. 9. Treibs subdivided them into reactions that readily occur and those that require harsher conditions, such as heat. Demetallation, ester hydrolysis, decarboxylation at the isocyclic ring, reduction of the vinyl group, and aromatization were considered to occur spontaneously, whereas ketone reduction and metal chelation would require harder conditions. Sedimentary porphyrins are almost always found as complexes with nickel(II) or oxovanadium(IV). Treibs also suggested a similar set of reactions for the diagenesis of heme (**10**) to produce nickel(II) and oxovanadium(IV) complexes of etio-type porphyrins, as shown in Fig. 10.[5,6,11,49,50]

Advancements over the years in the power and sensitivity of analytical techniques have enabled scientists to extract, purify, and elucidate the structures of porphyrins found in sediments, oil shales, and petroleum. Furthermore, many of the intermediates and their derivatives proposed by Treibs could be described and correlated to chlorophylls, bacteriochlorophylls, and heme. Other diagenetic pathways were suggested, including condensation or rearrangements to form five- or seven-membered isocycles,[6] and fusion with one or more benzene rings and/or aromatic heterocycles (*e.g.* thiophene).[9,51] These are collectively known as geoporphyrins or petroporphyrins and have been extensively reviewed.[5–9,11] Selected structures are shown in Fig. 11 along with their supposed biological origins.

The oldest record of fossil porphyrins (1.1 billion years old) was reported from extracts of marine sediments in Mauritania, West Africa. A mixture of nickel(II)- and oxovanadium(IV)-coordinated porphyrins were separated by reversed-phase HPLC-UV-

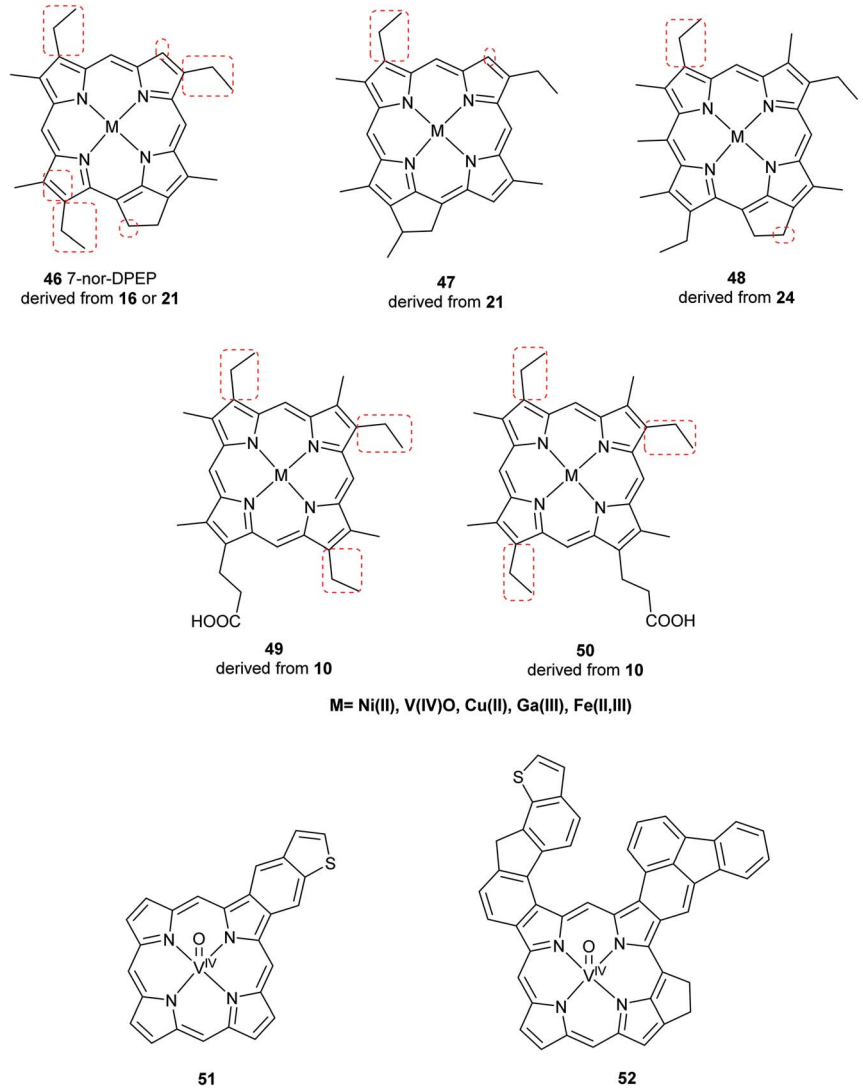

Fig. 11 Structures of selected sedimentary porphyrins, highlighting their differences to the natural porphyrins from which they are supposedly derived.

vis and identified by diode array detector and Fourier-transform cyclotron resonance mass spectrometry (Fig. 12). Nickel(II) porphyrins showed absorbance maxima at 400 and 550 nm, and the oxovanadium(IV) porphyrins showed peak maxima at 415 and 570 nm. They were later purified and their spectra compared to those of standard compounds. Their biological origin could not be correlated to a specific chlorophyll structure, although their origin was shown to be cyanobacterial.[1] Isotopic analysis of the sediment showed a composition of nitrogen-15 isotopes specific for cyanobacteria and different from those of algal and plant origins.[52,53] These findings support the predominance of cyanobacteria rather than algae in the Precambrian ocean.[1]

Chlorophylls in the fossil record

Chlorophylls, bacteriochlorophylls, and their degradation products found in terrestrial (*e.g.*, petroleum) or marine sediments (*e.g.*, mud from the ocean bottom) have been more commonly described than heme-derived sedimentary porphyrins. The main pigments detected in such sediments include the chlorophyll derivatives **29–39**.[54]

The oldest record of fossil phorbin derivatives is the green pigment **37**, the methyl ester of **35** (see Fig. 8). It was identified in chloroform extracts of green-colored fossil leaves from the middle Eocene brown coals in Geiseltal near Halle, eastern Germany. Several techniques including UV-vis spectroscopy, infrared spectroscopy, paper chromatography, and mass spectrometry indicated the intact isocyclic ring of phorbin and confirmed the pigment's identity when compared to the spectra of standard compound **37**.[55] Fig. 13 shows a distinctly green-colored fossil leaf from the Geiseltal.[56] Seven years later, **37** was identified in the Oligocene to Miocene Succor Creek Flora (25–36 million years old) in Oregon, USA, from green-colored fossil *Zelkova*,[57] *Celtis*, and *Ulmus* leaves.[58] Interestingly, these findings indicated that the diagenesis of these chlorophyll derivatives, specifically in these two regions, was halted after demetallation (Fig. 9)[55,57] owing to anaerobic conditions,[55] the

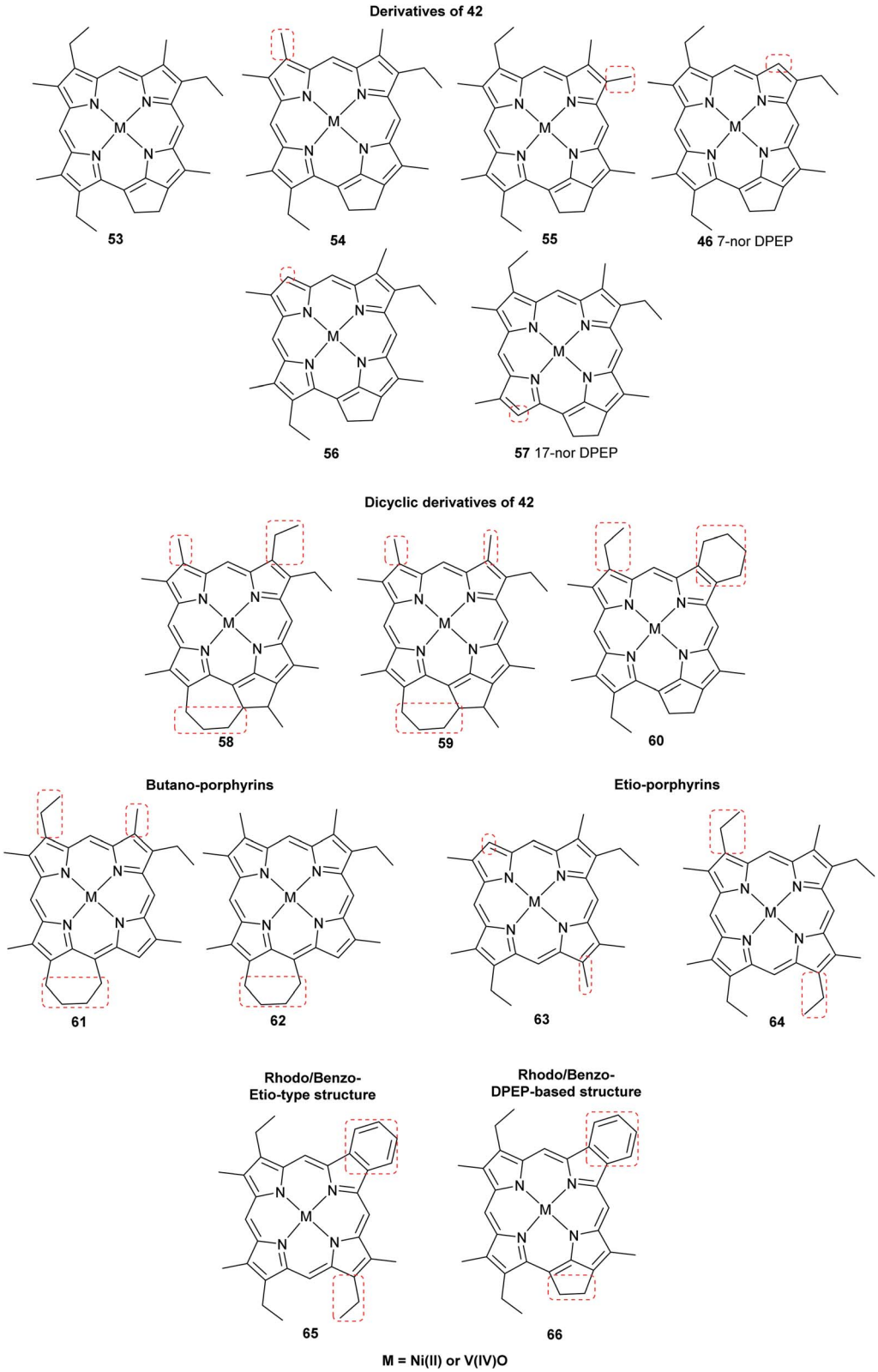

Fig. 12 Structures of the oldest reported porphyrins found as complexes with either nickel(II) or oxovanadium(IV). They are generally derived from chlorophylls.

Fig. 13 Green fossil leaf from the Eocene lignites in Geiseltal near Halle, eastern Germany, estimated to be around 46 million years old. It is deposited in the collections of the Naturkundemuseum Berlin, Germany. Based on its coloration, it is thought that chlorophyll or its diagenetic products would be present if extracted. Image taken by V. E. McCoy.

cold temperatures of coaly sediments,[55,58] and the absence of significant fluctuations in pH,[58] all of which promoted the preservation of chlorophylls and, accordingly, the green color of the leaves.

The chlorophyll metabolites **29** and **35** (Fig. 8) have been extracted and identified from well-preserved fossil leaves of *Platanus* spp., *Quercus* spp. and *Betula* spp. from the Miocene (15–22 million years old) deposits of the Clarkia Flora in North Idaho, USA. The fossils were shown to have intact chloroplasts among other ultrastructural organelles. These findings showed that, once again, chlorophyll diagenesis did not proceed to form alkylporphyrins. In contrast, the degraded chlorophyll derivative DPEP (**42**) and similar etioporphyrins were detected in fossil leaves of *Castanea* spp. and *Persea* spp. from the same deposits, in which no distinct organelles were preserved. These leaves may have been exposed to high temperatures or to oxidative conditions. No metal complexes were detected in any of the leaves.[59]

Conclusions & perspectives

Porphyrins comprise a large, diverse class of pigments that are present in a variety of plants and animals and play essential roles in the biochemistry of life. The major, biologically relevant (metallo)porphyrins include heme, protoporphyrin IX, chlorophylls, and bacteriochlorophylls. Porphyrins are able to resist decay, and their tetrapyrrole core structure often remains intact despite structural modifications upon fossilization. Knowledge of the chemical diagenetic pathways in combination with aspects related to the depositional environment of the fossil will facilitate future discoveries of porphyrins in fossils. Moreover, taphonomy studies would contribute to elucidating the degradation processes of these molecules under controlled conditions. The recent advancement of analytical techniques and the development of highly sensitive analytical instruments and methods will certainly promote future research and discoveries in this field. Molecular paleontology is a blossoming area which bears great promises to advance fossilization research.

Conflicts of interest

There are no conflicts to declare.

Acknowledgements

The authors have been funded by the Deutsche Forschungsgemeinschaft (DFG) as part of the DFG Research Unit FOR 2685 "The Limits of the Fossil Record: Analytical and Experimental Approaches to Fossilization" (grant numbers 396706817 to Carole T. Gee, 396703500 to Christa E. Müller, 3996637283 to Jes Rust for Victoria E. McCoy, and 396703500 to P. Martin Sander, respectively). This publication is contribution number 32 of FOR 2685.

References

1 N. Gueneli, A. M. McKenna, N. Ohkouchi, C. J. Boreham, J. Beghin, E. J. Javaux and J. J. Brocks, *Proc. Natl. Acad. Sci. U. S. A.*, 2018, **115**, E6978–E6986.
2 Z. Suo, R. Avci, M. H. Schweitzer and M. Deliorman, *Astrobiology*, 2007, **7**, 605–615.
3 L. R. Milgrom, *The Colours of Life: An Introduction to the Chemistry of Porphyrins and Related Compounds*, Oxford University Press, 1997.
4 K. M. Smith, in *Porphyrins and Metalloporphyrins: A New Edition Based on the Original Volume by J. E. Falk*, ed. K. M. Smith, Elsevier Scientific Publishing Company, Amsterdam, 1975, pp. 3–28.
5 B. J. Keely, W. G. Prowse and J. R. Maxwell, *Energy Fuels*, 1990, **4**, 628–634.
6 H. J. Callot, R. Ocampo and P. Albrecht, *Energy Fuels*, 1990, **4**, 635–639.
7 N. A. Mironov, D. V. Milordov, G. R. Abilova, S. G. Yakubova and M. R. Yakubov, *Pet. Chem.*, 2019, **59**, 1077–1091.
8 C. C. Naylor and B. J. Keely, *Org. Geochem.*, 1998, **28**, 417–422.
9 X. Zhao, C. Xu and Q. Shi, in *Structure and Modeling of Complex Petroleum Mixtures*, Springer, 2015, pp. 39–70.
10 E. Cappellini, A. Prohaska, F. Racimo, F. Welker, M. W. Pedersen, M. E. Allentoft, P. de Barros Damgaard, P. Gutenbrunner, J. Dunne, S. Hammann, M. Roffet-Salque, M. Ilardo, J. V. Moreno-Mayar, Y. Wang, M. Sikora, L. Vinner, J. Cox, R. P. Evershed and E. Willerslev, *Annu. Rev. Biochem.*, 2018, **87**, 1029–1060.

11 H. Falk and K. Wolkenstein, *Prog. Chem. Org. Nat. Prod.*, 2017, 52–59.
12 H. J. Kim, in *eLS*, John Wiley & Sons, Ltd, Chichester, UK, 2018, pp. 1–9.
13 J. W. Buchler, in *Porphyrins and Metalloporphyrins: A New Edition Based on the Original Volume by J. E. Falk*, ed. K. M. Smith, Elsevier Scientific Publishing Company, Amsterdam, 1975, pp. 157–231.
14 G. R. Seely, in *The Chlorophylls*, Elsevier, 1966, pp. 67–109.
15 R. Huszánk and O. Horváth, *Chem. Commun.*, 2005, 224–226.
16 U. Neugebauer, A. März, T. Henkel, M. Schmitt and J. Popp, *Anal. Bioanal. Chem.*, 2012, **404**, 2819–2829.
17 C. K. Lim, M. A. Razzaque, J. Luo and P. B. Farmer, *Biochem. J.*, 2000, **347**, 757–761.
18 M. Senge, A. Ryan, K. Letchford, S. MacGowan and T. Mielke, *Symmetry*, 2014, **6**, 781–843.
19 H. K. Lichtenthaler and C. Buschmann, *Curr. Protoc. Food Anal. Chem.*, 2001, **1**, F4.3.1–F.4.3.8.
20 L. Pilon and H. Berberoğlu, in *Handbook of Hydrogen Energy*, CRC Press, Boca Raton, 2014, pp. 369–418.
21 A. P. Razjivin, E. P. Lukashev, V. O. Kompanets, V. S. Kozlovsky, A. A. Ashikhmin, S. V. Chekalin, A. A. Moskalenko and V. Z. Paschenko, *Photosynth. Res.*, 2017, **33**, 289–295.
22 M. H. Schweitzer, *Annu. Rev. Earth Planet. Sci.*, 2011, **39**, 187–216.
23 G. Eglinton and G. A. Logan, *Philos. Trans. R. Soc., B*, 1991, **333**, 315–328.
24 N. L. Huq, S. M. Rambaud, L. C. Teh, A. D. Davies, B. McCulloch, M. M. Trotter and G. E. Chapman, *Biochem. Biophys. Res. Commun.*, 1985, **129**, 714–720.
25 N. V. Bhagavan and C.-E. Ha, in *Essentials of Medical Biochemistry*, Elsevier, 2015, pp. 511–529.
26 K. E. Anderson and S. Collins, *Am. J. Med.*, 2006, **119**, 801.e19, DOI: 10.1016/j.amjmed.2006.05.026.
27 M. H. Schweitzer, M. Marshall, K. Carron, D. S. Bohle, S. C. Busse, E. V. Arnold, D. Barnard, J. R. Horner and J. R. Starkey, *Proc. Natl. Acad. Sci. U. S. A.*, 1997, **94**, 6291–6296.
28 D. E. Greenwalt, Y. S. Goreva, S. M. Siljeström, T. Rose and R. E. Harbach, *Proc. Natl. Acad. Sci. U. S. A.*, 2013, **110**, 18496–18500.
29 J. Lindgren, T. Kuriyama, H. Madsen, P. Sjövall, W. Zheng, P. Uvdal, A. Engdahl, A. E. Moyer, J. A. Gren, N. Kamezaki, S. Ueno and M. H. Schweitzer, *Sci. Rep.*, 2017, **7**, 1–13.
30 P. O. Carra, in *Porphyrins and Metalloporphyrins: A New Edition Based on the Original Volume by J. E. Falk*, ed. K. M. Smith, Elsevier Scientific Publishing Company, Amsterdam, 1975, pp. 123–153.
31 G. Y. Kennedy and H. G. Vevers, *Comp. Biochem. Physiol., Part B: Biochem. Mol. Biol.*, 1976, **55**, 117–123.
32 M. Huang, H. Hu, L. Ma, Q. Zhou, L. Yu and S. Zeng, *Drug Metab. Rev.*, 2014, **46**, 362–378.
33 R. B. Frydman and B. Frydman, *Acc. Chem. Res.*, 1987, **20**, 250–256.
34 M. J. Terry, in *Heme, Chlorophyll, and Bilins*, ed. A. Smith and M. Witty, Humana Press, 2002, pp. 273–291.
35 A. Gorchein, C. K. Lim and P. Cassey, *Biomed. Chromatogr.*, 2009, **23**, 602–606.
36 B. Igic, D. R. Greenwood, D. J. Palmer, P. Cassey, B. J. Gill, T. Grim, P. L. R. Brennan, S. M. Bassett, P. F. Battley and M. E. Hauber, *Chemoecology*, 2010, **20**, 43–48.
37 D. B. Thomas, M. E. Hauber, D. Hanley, G. I. Waterhouse, S. Fraser and K. C. Gordon, *J. Exp. Biol.*, 2015, **218**, 2670–2674.
38 J. Wiemann, T. R. Yang, P. N. Sander, M. Schneider, M. Engeser, S. Kath-Schorr, C. E. Müller and P. M. Sander, *PeerJ*, 2017, **2017**, 1–20.
39 A. Gossauer and N. Engel, *J. Photochem. Photobiol., B*, 1996, **32**, 141–151.
40 A. Ben-Shem, F. Frolow and N. Nelson, *Nature*, 2003, **426**, 630–635.
41 H. Scheer, in *Chlorophylls and Bacteriochlorophylls*, Springer Netherlands, 2006, pp. 1–26.
42 A. N. Melkozernov and R. E. Blankenship, in *Chlorophylls and Bacteriochlorophylls*, Springer Netherlands, 2006, pp. 397–412.
43 M. Roca, K. Chen and A. Perez-Galvez, in *Handbook on Natural Pigments in Food and Beverages: Industrial Applications for Improving Food Color*, ed. R. Carle and R. Schweiggert, Woodhead Publishing, 2016, pp. 125–158.
44 J. L. Thweatt, D. P. Canniffe and D. A. Bryant, in *Advances in Botanical Research*, 2019, pp. 35–89.
45 K. G. Wallace, J. Rimmer, S. K. Manley, J. F. Unsworth, A. H. Jackson and N. Albert, *Philos. Trans. R. Soc., B*, 1976, **273**, 255–276.
46 S. Hörtensteiner, *Cell. Mol. Life Sci.*, 1999, **56**, 330–347.
47 S. Hörtensteiner, *Annu. Rev. Plant Biol.*, 2006, **57**, 55–77.
48 J. D. Barnes, L. Balaguer, E. Manrique, S. Elvira and A. W. Davison, *Environ. Exp. Bot.*, 1992, **32**, 85–100.
49 A. E. Treibs, *Angew. Chem.*, 1936, **49**, 682–686.
50 A. E. Treibs, *Justus Liebigs Ann. Chem.*, 1934, **510**, 42–62.
51 K. Qian, T. R. Fredriksen, A. S. Mennito, Y. Zhang, M. R. Harper, S. Merchant, J. D. Kushnerick, B. M. Rytting and P. K. Kilpatrick, *Fuel*, 2019, **239**, 1258–1264.
52 M. B. Higgins, F. Wolfe-Simon, R. S. Robinson, Y. Qin, M. A. Saito and A. Pearson, *Geochim. Cosmochim. Acta*, 2011, **75**, 7351–7363.
53 J. M. Fulton, M. A. Arthur and K. H. Freeman, *Global Biogeochem. Cycles*, 2012, **26**, 1–15.
54 T. S. Bianchi and E. A. Canuel, in *Chemical Biomarkers in Aquatic Ecosystems*, Princeton University Press, 2011.
55 D. L. Dilcher, R. J. Pavlick and J. Mitchell, *Science*, 1970, **168**, 1447–1449.
56 C. T. Gee and V. E. McCoy, in *Fossilization: Understanding the Material Nature of Ancient Plants and Animals*, ed. C. T. Gee, V. E. McCoy, and P. M. Sander, Johns Hopkins University Press, Baltimore, 2021.
57 K. J. Niklas and D. E. Giannasi, *Science*, 1977, **196**, 877–878.
58 D. E. Giannasi and K. J. Niklas, *Science*, 1977, **197**, 765–767.
59 K. J. Niklas and R. M. Brown, *Am. J. Bot.*, 1981, **68**, 332–341.